

# A Quality Analysis on JPEG 2000 Compressed Leukocyte Images by Means of Segmentation Algorithms

Alexander Falcón-Ruiz<sup>1</sup>, Juan Paz-Viera<sup>1</sup>,  
Alberto Taboada-Crispi<sup>1</sup>, and Hichem Sahli<sup>2</sup>

<sup>1</sup> Center for Studies on Electronics and Information Technologies, Universidad Central de Las Villas, Carretera a Camajuaní km 5 ½, Santa Clara, VC, CP 58430, Cuba

{afalcon, jpaz, ataboada}@uclv.edu.cu

<sup>2</sup> Vrije Universiteit Brussel, Dept. Electronics & Informatics, VUB-ETRO,  
B-1050 Brussels, Belgium

sahli@etro.vub.ac.be

**Abstract.** Reducing image file size by means of lossy compression algorithms can lead to distortions in image content affecting detection of fine detail structures, either by human or automated observation. In the case of microscopic images of blood cells, which usually occupy large amounts of disk space, the use of such procedures is justified within a controlled quality loss. Although JPEG 2000 remains as the accepted standard for lossy compression, still a set of guidelines need to be established in order to use this codec in its lossy mode and for particular applications. The present paper deals with a quality analysis of reconstructed microscopic leukocytes images after they have been lossy compressed. The quality loss is investigated near the lower compression bound by evaluating the performance of several segmentation algorithms together with objective quality metrics. The value of compression rate of 142:1 is estimated from the experiments.

**Keywords:** microscopic images, leukocytes, segmentation, JPEG 2000, compression.

## 1 Introduction

Images produced by digital microscopy techniques are characterized by large file sizes due, not only to the bit depths employed, but also to the high resolution properties of the digital acquisition devices. The amount of such images obtained in daily practice, also depending on the type of studies required for every particular detection task, can be huge, leading to problems of storage and transmission of the image data through communication networks [1], [2].

Reducing file size of microscopic images by means of lossy compression algorithms, such as the JPEG 2000 codec, can lead to image distortions and therefore, to affect their value for diagnosis. Preservation of image quality is essential, for example, the count of white blood cell (leukocyte) structures within the observed field of view can lead to identification and/or diagnosis of several pathologies, such as acquired immunodeficiency syndrome, cancers, or chronic infections. Fig. 1a) shows a typical image where leukocytes are indicated. The fine detail structures, which

identify or differentiate among the different leukocyte types, are sensitive to distortions, such as noise or artifacts introduced by *lossy* codecs.

The JPEG 2000 codec (ISO 15444-1) uses the Wavelet Transform as the kernel transformation surpassing the performance of its predecessor, the JPEG codec, based on Discrete Cosine Transform [3], [4]. *Lossy* codecs have been reported as having compression ratio (CR) of one order of magnitude higher than those obtained with *lossless* ones.

Although JPEG2000 has been adopted by DICOM standard, there are still no regulations for the use of its *lossy* mode where the higher the CRs are, the more distortion is introduced in the image, affecting particularly edge definition and therefore, jeopardizing the correct identification of the structures and the diagnosis made through these images [5]. Fig. 1 show Regions of Interest (ROIs) containing two different types of leukocytes, i.e. monocyte and lymphocyte, extracted from image in Fig. 1a) after compression at different CRs.

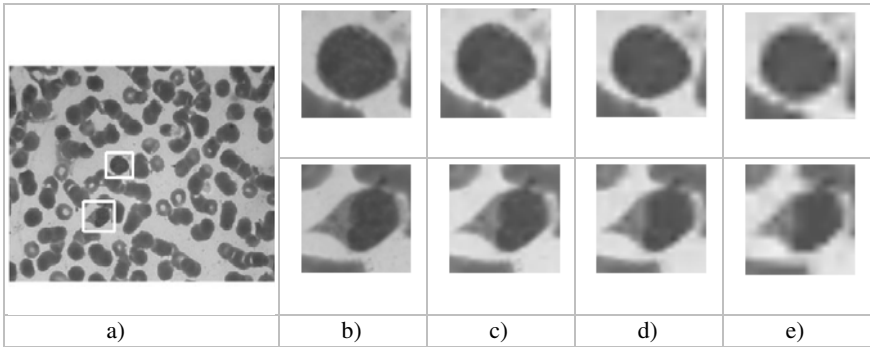


**Fig. 1.** Image in a) shows a bitmap of 1536V x 2048H pixel size, which occupies 9.00 MB of disk space. White squares indicate two different types of leukocytes, i.e. lymphocyte and monocyte. Images in columns b) to e) show the two leukocytes extracted from image in column a) compressed at different CRs; b) no compression, c) CR=250:1, d) CR=500:1 and e) CR=1000:1. The edges, texture and contrast are severely distorted as compression rate increases.

Several researches have been carried out in order to establish a CR limit for specific image types where the overall perceived image quality is not perceptually affected when using *lossy* codec [6], [7], [8]. In this paper, we propose a strategy to estimate the maximum allowable CR where deterioration introduced in the images by the codec, does not affect the quality of leukocytes images. The estimation is based on the performance of several segmentation algorithms.

## 2 Materials and Methods

### 2.1 The Images

Images were acquired using a Micrometrics 318CU CMOS digital camera, resulting in 24-bit color pictures of 2048H x 1536V size. The camera was attached to an

Accu-scope 3016PL trinocular microscope with 100x oil immersion objective and 10x eyepieces. For the test, we selected 15 images per leukocyte class, where the classes of interest were: lymphocytes, monocytes, neutrophils, basophils and eosinophils. Some manually cropped images are shown in Fig.2.

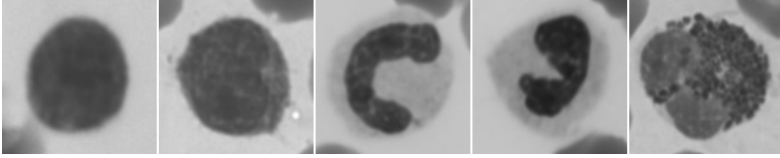


Fig. 2. Leukocytes. Left to right: lymphocyte, monocyte, neutrophil, basophil, eosinophil

## 2.2 Compression with JPEG 2000 Codec

For achieving JPEG2000 compression, the *JasPer* software [9] was employed. Images as in Fig. 1a) were compressed at 30 different compression factor (CF=1/CR), from 0.001 (CR=1000:1) to 0.03 (CR=33:1), with a step of 0.001. Then, ROIs were extracted from the uncompressed and the 30 compressed images.

The CR was calculated as the necessary memory space (in bytes) for allocating uncompressed image divided by the number of bytes necessary for allocating the same image in its compressed format.

## 2.3 The Segmentation Algorithms and Distance Measures

Typically, leukocytes identification is based on visual inspection of individual images with fields of view wider than the size of individual cells and containing other structures as well as noise and/or artifacts. The approach of having experts dedicated to this task is time consuming, exhausting and prone to human error, requiring frequent repetitions to validate results [11]. These situations, altogether with the great amount of images necessary to achieve a diagnosis, encourage scientists to develop segmentation algorithms as an early stage for automated classification.

Three automatic segmentation algorithms were tested over a set of leukocytes images each one compressed at 30 different CFs. These were the Otsu's method [12], Active Contours (AC) method [13] and the Mixture of Gaussians (MoG) method [14]. For assessing the segmentation results, of each of the proposed methods, applied at a specific CF, the contour based Hausdorff distance [15] and the region based Vinet distance [16], between Ground Truths (GTs) and segmentation results have been estimated. GTs were manually selected in each ROI at initial state, i.e. without compression.

Given two finite point sets  $A = \{a_1, \dots, a_p\}$  and  $B = \{b_1, \dots, b_q\}$ , the Hausdorff distance is defined as

$$H(A, B) = \max(h(A, B), h(B, A)) \quad (1)$$

where

$$h(A, B) = \max_{a \in A} \min_{b \in B} \|a - b\|, \quad (2)$$

and  $\|\cdot\|$  is some underlying norm on the points of A and B (e.g., the  $L_2$  or Euclidean norm). Thus, it measures the maximum mismatch between two sets by measuring the distance of the point of A that is farthest from any point of B and vice versa.

The Vinet distance between two images is computed as

$$s(L_i^n, R_j^n) = \sum_{p=1}^q \omega_p s_p(L_i^n, R_j^n), \quad (3)$$

for weight  $\omega_p$  and various resemblance functions between regions

$$s_p(L, R) = 1 - \frac{\min(A_p(L), A_p(R))}{\max(A_p(L), A_p(R))}, \quad (4)$$

where  $L_i^n, R_j^n$  are regions in the left ( $L$ ) and right ( $R$ ) images respectively and  $A_p$  is some attribute of a region, for example, intensity mean, intensity variance, special moment, etc.

## 2.4 Quantitative Measures

For our particular research the following bi-variate measures were calculated in order to have an estimate of image quality according to CF[1], [2], [10]:

- The Peak Signal-to-Noise Ratio (*PSNR*): considering  $X(i,j)$  as the uncompressed image and  $Y(i,j)$  the restored one, *PSNR* is defined as:

$$PSNR(dB) = 10 \cdot \log_{10} \left( \frac{MAXp^2}{MSE} \right), \quad (5)$$

where  $MAXp = 2^B - 1$ ,  $B$  is the image bitdepth and *MSE* (mean square error) is defined as:

$$MSE = \frac{1}{m \cdot n} \sum_{i=1}^m \sum_{j=1}^n (X(i,j) - Y(i,j))^2, \quad (6)$$

where  $m$  and  $n$  are the number of rows and columns in the image, respectively.

- The spectral distance (*SD*): a measure of distance between uncompressed and reconstructed Fourier domain images given by:

$$SD = \frac{1}{m \cdot n} \sum_{i=1}^m \sum_{j=1}^n (|\varphi(i,j)| - |\hat{\varphi}(i,j)|)^2, \quad (7)$$

where  $\varphi(i,j)$  and  $\hat{\varphi}(i,j)$  are the imaginary parts of Fourier transforms of uncompressed and restored images, respectively.

- The gain in Contrast to Noise ratio (*gCNR*) is defined as:

$$gCNR(dB) = 10 \cdot \log_{10} \left( \frac{CNR_X}{CNR_Y} \right), \quad (8)$$

where  $CNR_X$  and  $CNR_Y$  are the contrast-to-noise ratios in the uncompressed and reconstructed images respectively calculated as  $CNR_i = (\bar{X}_{i2} - \bar{X}_{i1}) / \sigma_i$ , with  $\bar{X}_{i1}$  and  $\bar{X}_{i2}$  being the mean values of intensity from two different regions in the  $i$ -th image and  $\sigma_i$  the standard deviation of noise in the same image.

- The structural similarity index (*MSSIM*): a powerful measure proposed by Wang *et al.* [10] was also employed. It can be calculated as:

$$MSSIM(X, Y) = \frac{1}{M} \sum_{i=1}^M SSIM(x_i, y_i), \tag{9}$$

where  $M$  is the number of image blocks  $x_i$  and  $y_i$  of uncompressed and reconstructed image respectively and  $SSIM$  calculated as:

$$SSIM(X, Y) = \frac{(2\mu_X\mu_Y + C_1)(2\tau_{XY} + C_2)}{(\mu_X^2 + \mu_Y^2 + C_1)(\tau_X^2 + \tau_Y^2 + C_2)}, \tag{10}$$

where  $\mu_X$  and  $\mu_Y$  are the luminance values,  $\tau_X$  and  $\tau_Y$  the contrast estimation values for uncompressed and reconstructed images respectively, and  $\tau_{XY} = \frac{1}{N-1} \sum_{i=1}^N (x_i - \mu_X)(y_i - \mu_Y)$ . The constants  $C_1$  and  $C_2$  are placed to avoid instability:  $C_i = (K_i L)^2$  where  $L = 255$ , for 8bpp images and  $K_i \ll 1$ .

All bi-variate calculations are made between the uncompressed image and every reconstructed image after being compressed at each CF value in the interval studied.

### 3 Results

The normalized Hausdorff distances for the three segmentation algorithms tested are shown in Fig. 3. As we can see, the three methods show a similar behavior as quality metrics, with Otsu’s method having lower Hausdorff distance to the GT in general. The Hausdorff distance for CF higher than 1/142, has a standard deviation below 5% of the Hausdorff distance for the maximum CR tested.

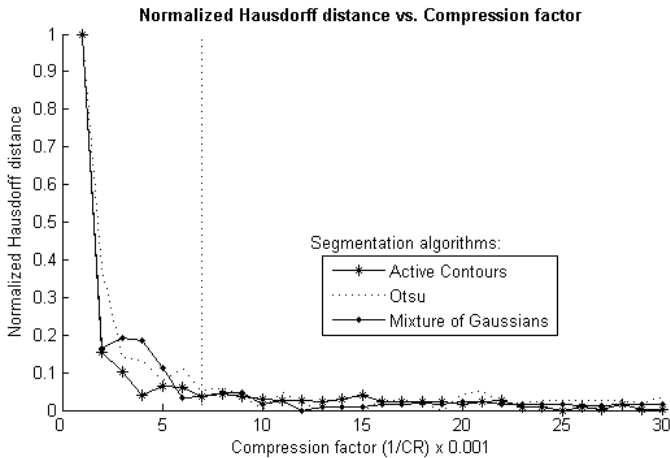


**Fig. 3.** Normalized Hausdorff distance (HD) for the three segmentation algorithms tested. Dotted line at CF=0.007(CR=142:1) indicates the estimated lower bound, at this point not normalized  $HD_{AC} = 10.3$ ,  $HD_{Otsu} = 4.5$  and  $HD_{MoG} = 8.3$  Hausdorff distance units.

Fig. 4 shows the normalized Vinet distances for the three segmentation algorithms. In this case, the curves are smoother; due to Vinet distance capture better perturbation in edge (introduced by JPEG2000 Codec) than Hausdorff distance, which is more tolerant to those variations, because it measures proximity rather than exact superposition.

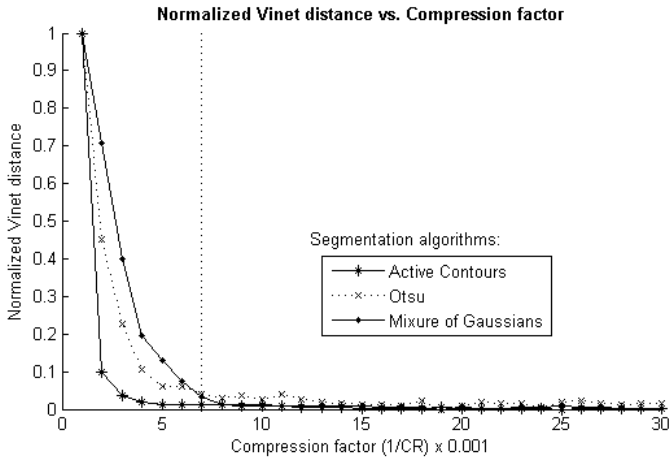


**Fig. 4.** Normalized Vinet distance (VD) for the three segmentation algorithms tested. Dotted line at  $CF=0.007(CR=142:1)$  indicates the estimated lower bound, at this point not normalized $HD_{AC} = 1.0$ ,  $VD_{Otsu} = 1.1$  and  $VD_{MoG} = 2.3$  Vinet distance units.

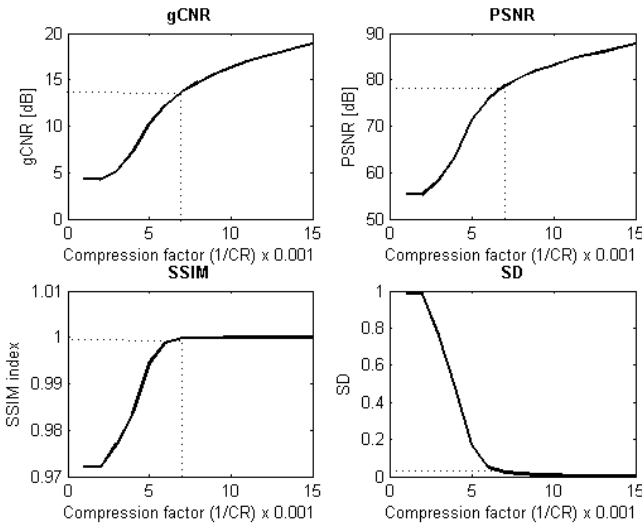


**Fig. 5.** The calculated objective metrics are shown in a compression interval from 1 to 15. At  $CF=0.007(CR=142:1)$ ,  $gCNR=13.7$  dB,  $PSNR=78.7$  dB,  $SSIM = 0.99$  and  $SD=0.02$ .

The nick point in the curves at  $CF=0.007$  ( $CR=142:1$ ) suggests a lower CR bound. For CR values bigger than this, image quality is severely distorted, as we can corroborate in Fig. 5 with quantitative measures. At this CR, file size is reduced from 9 MB to approximately 65 KB. Metrics such as PSNR and gCNR show a stronger dependency with variation in CR while metrics such as SD and SSIM show less dependence with CR.

## 4 Conclusions

The analysis with the automatic segmentation algorithms tested suggested an interval of CR values from 33:1 up to 142:1 where is *safe* to use JPEG 2000. This initial and partial result is later confirmed by objective metrics, which agrees in the upper most CR value of 142:1.

Both, metrics for evaluating the performance of segmentation algorithms and objective quality distortion, are considered representative for estimating quality degradation caused by the *lossy* codec.

The result presented are preliminary and lack of subjective experience in interpreting this type of images. A more complex investigation including subjective evaluation should be carried out in order to precise the bounds for *lossy* compression. Nevertheless, a CR limit of 142:1 was estimated through both metric types as a limit for using JPEG 2000 compression in leukocytes identification tasks.

## Acknowledgements

The authors would like to thank, the Canadian International Development Agency Project Tier II-394-TT02-00 and the Flemish VLIR-UOS Programme for Institutional University Cooperation (IUC) for partly supporting this investigation.

## References

1. Acharya, T., Ray, A.K.: Image Processing Principles and Applications. John Wiley & Sons, Inc., Hoboken (2005)
2. Lau, C., et al.: Telemedicine. In: Kim, Y., Horri, S. (eds.) Handbook of Medical Imaging, vol. 3, pp. 305–331. SPIE, Bellingham (2000)
3. Clunie, D.A.: DICOM Supplement 61: JPEG 2000 Transfer Syntaxes (2002), [ftp://medical.nema.org/medical/dicom/final/sup61\\_ft.pdf](ftp://medical.nema.org/medical/dicom/final/sup61_ft.pdf)
4. Rabbani, M., Joshi, R.: An overview of the JPEG 2000 still image compression standard. 1, Signal Processing: Image Communication 17, 3–48 (2002)
5. Foes, D.H., et al.: JPEG 2000 compression of medical imagery. In: Proc. SPIE, San Diego, California, vol. 3980 (2002)
6. Penedo, M., Lado, M.J., Tahoces, P.G., Souto, M., Vidal, J.J.: Effects of JPEG 2000 data compression on an automated system for detecting clustered microcalcifications in digital mammograms. IEEE Trans. on Information Technology in Biomedicine 10(2) (2006)
7. Zhang, Y., Pham, B., Eckstein, M.P.: Evaluation of JPEG 2000 encoder options: human and model observer detection of variable signals in X-Ray coronary angiograms. IEEE Trans. On Med. Imaging 23(5) (2004)
8. Paz, J., Pérez, M., Schelkens, P., Rodríguez, J.: Impact of JPEG 2000 Compression on Lesion Detection in MR Imaging. Journal of Medical Physics 36(11), 4967–4976 (2009)
9. Adams, M., Kossentini, F.: JasPer: a software based JPEG 2000 codec implementation. In: Proc. of IEEE International Conference on Image Processing, vol. 2, pp. 53–56. Institute of Electrical and Electronics Engineers, Vancouver, British Columbia, Canada (2002)
10. Wang, Z., Bovik, A.C., Sheikh, H.R., Simoncelli, E.P.: Image Quality Assessment: From Error Visibility to Structural Similarity. IEEE Trans. on Image Proc. 13(4) (2004)

11. Lee, J.K.T.: Interpretation accuracy and pertinence. *American College of Radiology* 4 (2002)
12. Otsu, N.: A Threshold Selection Method from Gray-Level Histograms. *IEEE Transactions on Systems, Man and Cybernetics* 9(1), 62–66 (1979)
13. Kass, M., Witkin, A., Terzopoulos, D.: Snakes: Active contour models. *International Journal of Computer Vision* 1(4), 321–331 (1988)
14. Gupta, L., Sortrakul, T.: A gaussian-mixture-based image segmentation algorithm. *Pattern Recognition* 31(3), 315–325 (1998)
15. Huttenlocher, D., Klanderman, G.A., Rucklidge, W.J.: Comparing Images Using the Hausdorff Distance. *IEEE Transactions on Pattern Analysis and Machine Intelligence* 15(9), 850–863 (1993)
16. Cohen, L., Vinet, L., Sander, P.T., Gagalowicz, A.: Hierarchical Regional Based Stereo Matching. In: *Proc. Computer Vision and Pattern Recognition*, pp. 416–421 (1989)